

# On the Origin of Pluto's Small Satellites by Resonant Transport

W. H. Cheng<sup>a</sup>, S. J. Peale<sup>b</sup>, Man Hoi Lee<sup>a,c</sup>

<sup>a</sup>*Department of Earth Sciences, The University of Hong Kong, Pokfulam Road, Hong Kong*

<sup>b</sup>*Department of Physics, University of California, Santa Barbara, CA 93106, United States*

<sup>c</sup>*Department of Physics, The University of Hong Kong, Pokfulam Road, Hong Kong*

## ABSTRACT

The orbits of Pluto's four small satellites (Styx, Nix, Kerberos, and Hydra) are nearly circular and coplanar with the orbit of the large satellite Charon, with orbital periods nearly in the ratios 3:1, 4:1, 5:1, and 6:1 with Charon's orbital period. These properties suggest that the small satellites were created during the same impact event that placed Charon in orbit and had been pushed to their current positions by being locked in mean-motion resonances with Charon as Charon's orbit was expanded by tidal interactions with Pluto. Using the Pluto-Charon tidal evolution models developed by Cheng et al. (2014), we show that stable capture and transport of a test particle in multiple resonances at the same mean-motion commensurability is possible at the 5:1, 6:1, and 7:1 commensurabilities, if Pluto's zonal harmonic  $J_{2P} = 0$ . However, the test particle has significant orbital eccentricity at the end of the tidal evolution of Pluto-Charon in almost all cases, and there are no stable captures and transports at the 3:1 and 4:1 commensurabilities. Furthermore, a non-zero hydrostatic value of  $J_{2P}$  destroys the conditions necessary for multiple resonance migration. Simulations with finite but minimal masses of Nix and Hydra also fail to yield any survivors. We conclude that the placing of the small satellites at their current orbital positions by resonant transport is extremely unlikely.

## 1. INTRODUCTION

Pluto has five known satellites Charon, Styx, Nix, Kerberos, and Hydra, in the order of distance from Pluto. Charon was discovered in 1978 (Christy and Harrington 1978), Nix and Hydra in 2005 (Weaver et al. 2006), and Kerberos and Styx in 2011 and 2012 (Showalter et al. 2011, 2012). Charon is much larger than the other four satellites, and Nix and Hydra are in turn larger than Kerberos and Styx.<sup>1</sup> The system has nearly coplanar orbital geometry. The orbital periods are nearly in

---

<sup>1</sup> Kerberos and Styx are 10% and 4% as bright as Nix, respectively (Showalter et al. 2011, 2012), which means that they are  $\sim 30$  and 100 times less massive than Nix, if they have similar densities and albedos.

the ratios of 1:3:4:5:6, but sufficiently distinct from integer ratios relative to Charon that the small satellites are not in mean-motion resonances (MMR) with Charon (e.g., Buie et al. 2013). The orbits of the four small satellites are significantly non-Keplerian because of the large Charon-Pluto mass ratio ( $q = 0.1165$ ) and, at least in the case of Nix and Hydra, because of the additional effects of their proximity to the 3:2 mean-motion commensurability (Lee and Peale 2006). Orbits too close to Charon are unstable, and Styx is located near the inner edge of the stable region (Stern et al. 1994; Nagy et al. 2006). Orbits can also be destabilized by Nix and Hydra, and Kerberos is located in the only stable region between Nix and Hydra (Pires Dos Santos et al. 2011; Youdin et al. 2012).

The most likely scenario for the formation of Charon is a glancing impact where the impactor came off nearly intact in an eccentric orbit with semimajor axis near  $4R_P$  (where  $R_P$  is the radius of Pluto), with Pluto spinning rapidly, consistent with the current angular momentum of the system (Canup 2005). If the small satellites formed simultaneously, they must end up at orbital radii beyond the 3:1 to 6:1 mean-motion commensurabilities if they are to be captured and transported in resonances at these commensurabilities as Charon’s orbit tidally expanded to its current semimajor axis of  $17R_P$ .

For coplanar orbits, the lowest order terms in the disturbing function that can be resonant at the  $m+1:1$  mean-motion commensurability exterior to Charon are the following (Murray and Dermott 1999):

$$\Phi_m = \frac{GM_C}{a} \sum_{l=0}^m f_{m,l}(\alpha) e^{m-l} e_C^l \cos \phi_{m,l}, \quad (1)$$

where the resonance variables are

$$\phi_{m,l} = (m+1)\lambda - \lambda_C - (m-l)\varpi - l\varpi_C, \quad (2)$$

$G$  is the gravitational constant,  $M_C$  is the mass of Charon,  $a$ ,  $e$ ,  $\lambda$ , and  $\varpi$  are the orbital semimajor axis, eccentricity, mean longitude, and longitude of periapse of the small satellite, and the orbital elements with the subscript C are those of Charon. The quantities  $f_{m,l}$  are functions of  $\alpha = a_C/a$ , the Laplace coefficients, and their derivatives with respect to  $\alpha$ , whose forms are given in Appendix B of Murray and Dermott (1999) for  $m \leq 4$  using a different subscript notation for  $f$ .

The motion within each individual resonance term can be represented by a pendulum equation, where the coefficient of the cosine term in the disturbing function appears in the restoring acceleration (e.g., Murray and Dermott 1999). Any resonance variable can then be either circulating or librating about a constant value, but the latter can occur only if the eccentricity factors are non-zero. A problem with pushing the small satellites out in MMR with Charon is that the eccentricity of the small satellite rapidly increases to the point where the system becomes unstable if the resonance is one of the  $l \neq m$  Lindblad resonances containing powers of  $e$  in the coefficient of the restoring torque (e.g., Ward and Canup 2006).

One notes, however, that there is one resonance term with  $l = m$  in each set (Eq. [1]) that only contains powers of  $e_C$  in the coefficient. These are called corotation resonances, because the

perturbed satellite librates in a potential field that co-rotates with Charon. Ward and Canup (2006) took advantage of this and proposed to transport Nix and Hydra in corotation resonances at the 4:1 and 6:1 commensurabilities, where the eccentricity does not grow, and where the resonances are destroyed as  $e_C \rightarrow 0$  as the current dual synchronous equilibrium configuration of Pluto-Charon is approached. But Lithwick and Wu (2008) showed that the necessary conditions for migrating each satellite in a corotation resonance cannot be satisfied for Nix and Hydra simultaneously under the same assumptions used by Ward and Canup (i.e., zero gravitational harmonic coefficient  $J_{2P}$  of Pluto,<sup>2</sup> zero mass for Nix and Hydra, and imposed expansion of Charon’s orbit.)

Here we investigate the possible transport of the small satellites locked in multiple MMRs at the same commensurability, as Charon’s orbit is expanded according to conventional tidal models. Cheng et al. (2014, hereafter paper I) have studied in detail the tidal evolution of Pluto-Charon in two tidal models with the frequency  $f$  dependence of the dissipation function  $Q \propto 1/f$  or  $Q = \text{constant}$ , including dissipation in both Pluto and Charon and the possibility of permanent deviations from axisymmetry in both bodies. We showed in paper I that the inclusion of the effects of the gravitational harmonic coefficient  $C_{22C}$  of Charon (see footnote 2) for both rotational and orbital motions can have a profound effect on the orbital evolution when Charon is captured into spin-orbit resonances during the evolution.<sup>3</sup>

In Section 2 we demonstrate simultaneous capture in all or several of the resonances at the 5:1, 6:1, and 7:1 commensurabilities under the same assumptions used by Ward and Canup (2006) and Lithwick and Wu (2008), where  $J_{2P} = 0$  and the small satellites are treated as test particles, but with a more realistic tidal expansion of the orbit of Charon. The eccentricity of Charon’s orbit remains non-zero throughout most of the tidal evolution to the current configuration by a judicious choice of the ratio of tidal dissipation in Charon to that in Pluto (paper I), thereby maintaining the stability of the resonances. In some cases, the eccentricity of the test particle does not grow during the transport, which would occur in single Lindblad resonance capture. Although this seems like a possible solution to the eccentricity growth problem and the unlikely selection of only corotation resonances as the small satellites encounter the respective mean-motion commensurabilities with Charon, the test particle’s final eccentricity is still too large, and we are unable to demonstrate a similar multiple-resonance migration at the 3:1 and 4:1 commensurabilities. In Section 3 we show how a non-zero  $J_{2P}$  destroys the migration stability we find for test particles for a large ensemble of plausible initial conditions. Finally, the Pluto system with non-zero, but minimal masses for Nix and Hydra is integrated in Section 4 for plausible ranges of parameters in a search for an overlooked configuration that could lead to resonant transport of Nix and Hydra. None are found. We summarize and discuss the significance of these results in Section 5.

---

<sup>2</sup> The gravitational harmonic coefficients  $J_2$  and  $C_{22}$  of a body of mass  $M$  and radius  $R$  are given by  $J_2 = [\mathcal{C} - (\mathcal{A} + \mathcal{B})/2]/(MR^2)$  and  $C_{22} = (\mathcal{B} - \mathcal{A})/(4MR^2)$ , where  $\mathcal{A} \leq \mathcal{B} \leq \mathcal{C}$  are the principal moments of inertia.

<sup>3</sup> A brief summary of some of the material in both paper I and this paper appeared in an extended abstract by Peale et al. (2011).

## 2. MULTI-RESONANCE CAPTURE AND TRANSPORT

We study the behavior of the debris from the collisional capture of Charon by adding test particles to the simulations of the tidal evolution of Pluto-Charon presented in paper I. We use the Wisdom-Holman (1991) integrator in the SWIFT<sup>4</sup> package (Levison and Duncan 1994), modified to simulate the tidal, rotational and axial-asymmetry effects for Pluto and Charon (see paper I for details). The Jacobi coordinates are adopted for the test particles, following Lee and Peale (2006). We use a slightly different division of the Hamiltonian into the Keplerian and perturbation parts, which is designed for integrations with comparable masses (such as Pluto-Charon) in a hierarchical system (Lee and Peale 2003; see also Beust 2003). All external perturbations from the Sun and the other planets are negligibly small.

We assume a typical outcome for the collisional capture of Charon, where Charon emerges with non-zero orbital eccentricity  $e_C$  and semimajor axis  $a_C = 4R_P$  (Ward and Canup 2006). Both Pluto and Charon would be spinning after the collision (with both spin axes assumed to be perpendicular to the orbit plane), where the total angular momentum is that of the current system. Charon’s spin contributes relatively little to the total angular momentum, and it evolves quickly to the asymptotic tidal spin rate (where the tidal torque averaged over an orbit vanishes), unless it is captured temporarily into spin-orbit resonances due to non-zero  $C_{22C}$ . For the simulations in this section, we assume  $J_{2P} = 0$ .

For the tidal model where the tidal distortion of a body responds to the perturbing body a short time  $\Delta t$  in the past, constant  $\Delta t$  leads to  $Q \propto 1/f$ , so we call the  $Q \propto 1/f$  model the constant  $\Delta t$  model. As shown in paper I, the eccentricity  $e_C$  of Charon’s orbit can be roughly constant during most of the tidal evolution with the appropriate ratio of tidal dissipation in Charon to that in Pluto characterized by

$$A_{\Delta t} = \frac{k_{2C}}{k_{2P}} \frac{\Delta t_C}{\Delta t_P} \left( \frac{M_P}{M_C} \right)^2 \left( \frac{R_C}{R_P} \right)^5 \approx \frac{\mu_P}{\mu_C} \frac{\Delta t_C}{\Delta t_P} \frac{R_C}{R_P}, \quad (3)$$

where the subscripts  $P$  and  $C$  denote Pluto and Charon, respectively,  $M_i$  is the mass, and  $R_i$  is the radius. The second degree potential Love number

$$k_{2i} = \frac{3/2}{1 + 19\mu_i/(2\rho_i g_i R_i)} \quad (4)$$

for an incompressible homogeneous sphere of radius  $R_i$ , rigidity  $\mu_i$ , density  $\rho_i$ , and surface gravity  $g_i$ . We have used the approximation  $k_{2i} \approx 3\rho_i g_i R_i/(19\mu_i)$ , valid for small solid body, in the last form of Eq. (3).

We perform integrations with a range of eccentricity evolution of Charon by varying initial  $e_C$  and  $A_{\Delta t}$ . Charon on a highly eccentric orbit would lead to close encounters with the test particles and destabilize the resonances. Hence we select the range of initial  $e_C$  from 0.05 to 0.3, in steps

---

<sup>4</sup>See <http://www.boulder.swri.edu/~hal/swift.html>.

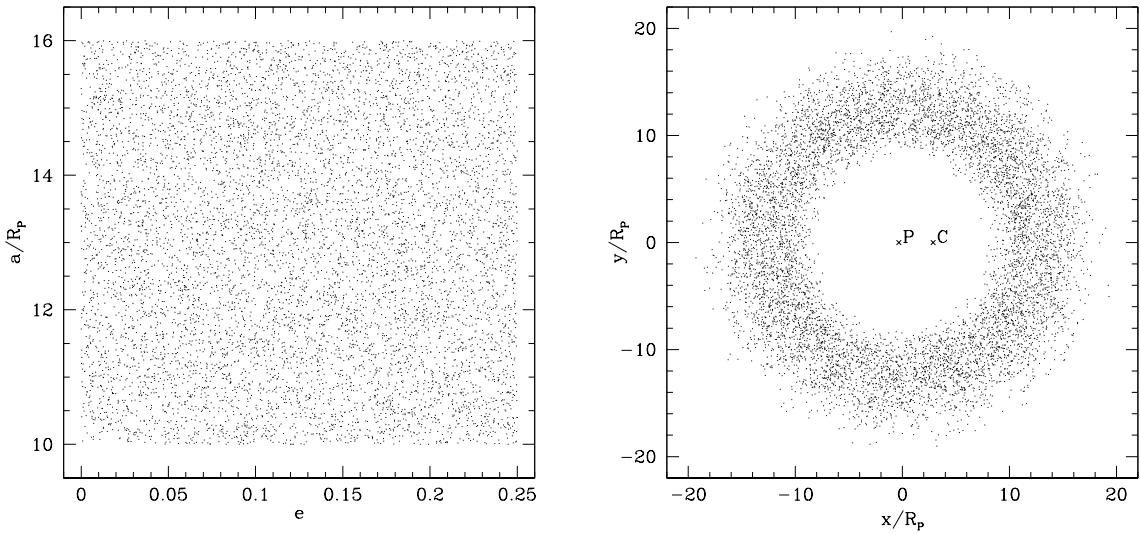


Fig. 1.— Initial distribution of the 8000 random test particles in  $(e, a)$  plane (left panel) and Cartesian  $(x, y)$  plane (right panel). The initial positions of Pluto and Charon with  $e_C = 0.2$  and Charon at periastron are shown as well in the right panel.

of 0.05. In these runs, we use  $k_{2P} = 0.058$  and  $\Delta t_P = 600$  seconds, same as that in paper I. The values of  $A_{\Delta t}$  are chosen to center at the value where  $e_C$  is roughly constant during most of the evolution:  $A_{\Delta t} = 9, 10,$  and  $11$ . Smaller (larger)  $A_{\Delta t}$  would result in  $e_C$  increasing (decreasing) throughout most of the evolution. We assume  $C_{22i} = 10^{-5}$ . For the constant  $\Delta t$  model, non-zero  $C_{22i}$  does not change the tidal evolution with initial  $e_C \leq 0.25$ . For initial  $e_C = 0.3$ , Charon can be captured into the 3:2 spin-orbit resonance, but the capture has only small effects on the evolution of  $a_C$  and  $e_C$  (see paper I). So we have not repeated the runs with  $C_{22i} = 0$ .

For each combination of initial  $e_C$  and  $A_{\Delta t}$ , 8000 test particles in orbits coplanar with that of Pluto-Charon are distributed with random initial conditions. The semimajor axis  $a$  spans from  $10R_P$  to  $16R_P$ , which corresponds to just within 4:1 up to 8:1 mean-motion ratio. The formation of a massive satellite together with a debris disk up to this extent by a single giant impact has been confirmed by high resolution SPH simulations (Canup 2011). The eccentricity  $e$  is between 0 and 0.25, and the longitude of periastron  $\varpi$  and mean anomaly  $\mathcal{M}$  are both randomly chosen. The initial  $(e, a)$  and  $(x, y)$  distributions of the test particles are shown in Fig. 1. The simulations are first run for  $10^{10}$  seconds ( $\approx 300$  years). We refer to this as the first stage of our integration.

Most of the test particles ( $\approx 99\%$ ) become unstable and are removed during the first stage of our integration. Test particles are removed if they have close encounter with either Pluto or Charon or get too far away ( $\gtrsim 100R_P$ ). About half of them are removed either very quickly without getting into any identifiable resonance with Charon, or as soon as they encounter one of the commensurabilities with Charon. A significant fraction of the latter are caught into a single

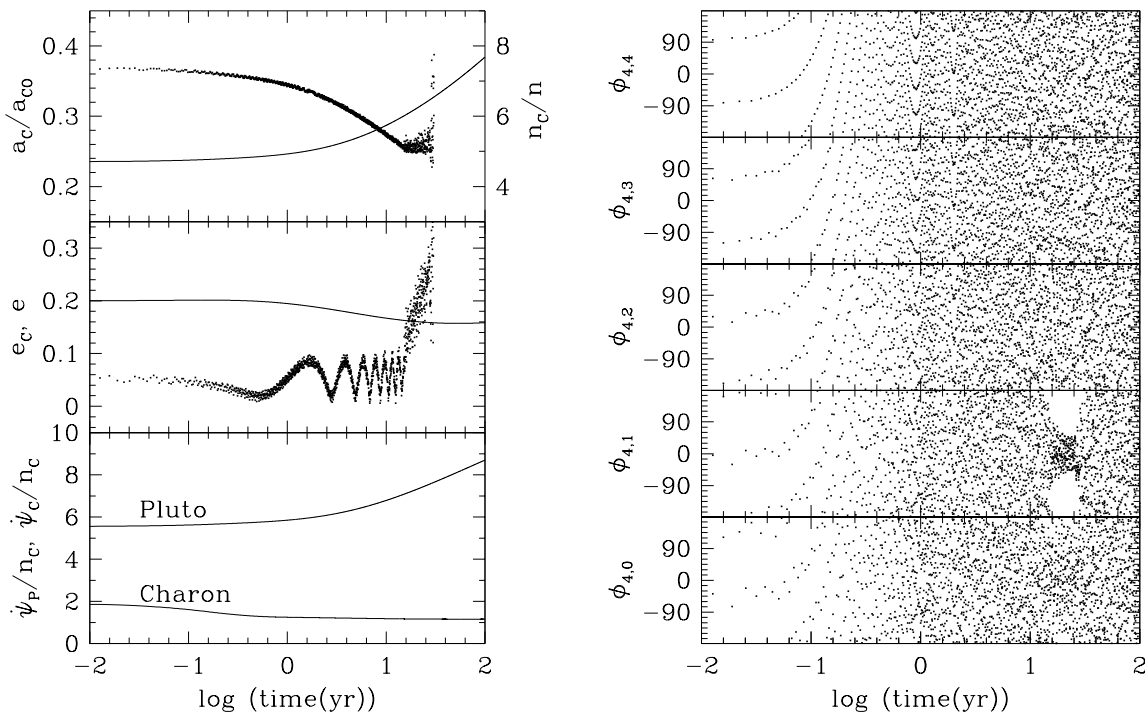


Fig. 2.— Example of a test particle captured into a single 5:1 Lindblad resonance with Charon in the constant  $\Delta t$  model. The panels show the evolution of Charon’s orbital semimajor axis  $a_C$  (in units of its current semimajor axis  $a_{C0}$ ) and eccentricity  $e_C$  and the spin angular velocities  $\dot{\psi}_i$  of Pluto and Charon (in units of Charon’s mean motion  $n_C$ ) as lines, and the evolution of  $e$ , the ratio of mean motion  $n_C/n$ , and the resonance variables  $\phi_{4,l}$  of the test particle as dots.  $e$  increases when  $\phi_{4,1}$  is librating, and the test particle becomes unstable.

Lindblad resonance between 4:1 and 8:1, which leads to excitation of their eccentricities. They become unstable and are removed eventually, as predicted by Ward and Canup (2006). We present one of these in Fig. 2 as an example. The figure shows the evolution of  $a_C$ ,  $e_C$ , and the spin angular velocities  $\dot{\psi}_i$  as lines, and the evolution of the orbital eccentricity  $e$ , mean motion ratio  $n_C/n$ , and resonance variables  $\phi_{4,l}$  (Eq. [2] with  $m = 4$ ) of the test particle as dots. Although Pluto’s spin is decreasing, the orbital mean motion is decreasing even faster so  $\dot{\psi}_P/n_C$  is rising. The orbital elements of the test particle are the osculating Keplerian ones in Jacobi coordinates. Before being captured, the period ratio decreases as  $a_C$  increases. After that, the ratio fluctuates around the value of that commensurability (5:1). Since Charon is massive and its orbit is eccentric, the orbit of the test particle is significantly non-Keplerian, as described by Lee and Peale (2006) and Leung and Lee (2013). The osculating Keplerian eccentricity  $e$  undergoes short period, small amplitude oscillations forced by the non-axisymmetric components of the potential of Pluto-Charon, and longer period oscillations from the superposition of the epicyclic motion and the forced eccentricity oscillation.  $e$

starts to grow as soon as the test particle is caught into a single  $m = 4$ ,  $l = 1$  Lindblad resonance, and the test particle becomes unstable and is removed when  $e$  becomes too high.

We have several tens of survivors in each simulation when we first stop the integrations, except for initial  $e_C = 0.05$ , where no particle survives. All of the survivors have been caught in multiple resonances at each mean-motion commensurability, which allow stable expansion of the test particle’s orbit as Charon’s orbit expands, but none of them are in 3:1 or 4:1. (Recall that Styx, Nix, Kerberos, and Hydra are near 3:1, 4:1, 5:1 and 6:1, respectively.) There were no captures into just the corotation resonances with subsequent stable expansion of the test particle orbit, and no stable expansions without simultaneous libration in multiple resonances at the same commensurability. In Table 1, we list the statistics of test particles remaining in 5:1, 6:1, and 7:1 resonances when we first stop the integrations. In a few cases, we find particles that have already escaped from multiple resonances at a mean-motion commensurability but not yet removed at the end of the first stage of our integration.

We observe a general trend that the fraction of captures into multiple 5:1 resonances decreases when initial  $e_C$  increases, and the opposite happens for 7:1 resonances. This trend and the result that no particle survives for initial  $e_C = 0.05$  can be understood qualitatively. If initial  $e_C$  is too small, the resonance widths are too narrow for simultaneous libration in multiple resonances. For 6:1, as we increase initial  $e_C$ , simultaneous libration in multiple resonances first becomes more stable as the resonance widths increase with  $e_C$ , but then becomes less stable when Charon comes too close at apopase and the perturbation from Charon becomes too strong. For the higher-order resonance 7:1 further from Charon, the fraction of captured test particles continues to increase up to initial  $e_C = 0.3$ . But for the lower-order resonance 5:1 closer to Charon, the fraction of captured test particles already decreases beyond initial  $e_C = 0.1$ . From this qualitative understanding of the trends in the numerical results, we believe we have focused on the suitable combinations of initial  $e_C$  and  $A_{\Delta t}$  in exploring the multiple resonance migration scenario.

We continue to integrate the particles that survive after our first stage of integration to the end of the tidal evolution of Pluto-Charon for the four corners and the middle point of the  $(e_C, A_{\Delta t})$  grid in Table 1. Most of the test particles escape from resonances and are removed, with the majority removed during the final decrease in  $e_C$  near the end of the tidal evolution. The final survived fractions of the initial 8000 test particles are summarized in Table 2.

Fig. 3 shows an example of a test particle that survives to the end of the tidal evolution of Pluto-Charon. The left panel shows the evolution of the semimajor axes, eccentricities, and spins as Charon’s semimajor axis expands from  $4R_P$  to its current value of  $17R_P$ , and the right panel shows the evolution of the six resonance variables  $\phi_{5,l}$  at the 6:1 commensurability with Charon. The test particle is captured into 6:1 resonance, with the simultaneous libration of all six resonance variables. The resonance variables alternate between libration about  $0^\circ$  and  $180^\circ$ , and the orbits are anti-aligned with the difference in the longitudes of periapse  $\varpi - \varpi_C = 180^\circ$ . The eccentricity of the test particle  $e$  does not exceed 0.2 for most of the evolution, when the eccentricity of Charon  $e_C$

Table 1. Fraction of captured test particles, in unit of permille (‰), after  $10^{10}$  seconds in the constant  $\Delta t$  model with  $C_{22i} = 10^{-5}$

Initial $e_C$	$A_{\Delta t} = 9$			$A_{\Delta t} = 10$			$A_{\Delta t} = 11$		
	5:1	6:1	7:1	5:1	6:1	7:1	5:1	6:1	7:1
0.10	7.75	2.50	0	9.63	0.63	0	6.00	0	0
0.15	1.00	11.00	4.13	4.25	9.38	3.00	5.75	10.25	2.50
0.20	0.88	6.88	5.00	1.25	8.75	5.38	3.13	11.13	4.89
0.25	0.25	4.38	6.13	0.75	4.00	6.00	0.50	7.38	5.88
0.30	0.25	4.13	6.13	0.50	3.25	7.38	0.25	4.88	6.75

Table 2. Fraction of survivors, in unit of permille (‰), to the end of the tidal evolution of Pluto-Charon in the constant  $\Delta t$  model with  $C_{22i} = 10^{-5}$ .

Initial $e_C$	$A_{\Delta t} = 9$			$A_{\Delta t} = 10$			$A_{\Delta t} = 11$		
	5:1	6:1	7:1	5:1	6:1	7:1	5:1	6:1	7:1
0.1	0	0.25	0	...	...	...	0	0	0
0.2	...	...	...	0	0.63	1.00	...	...	...
0.3	0	0.13	0	...	...	...	0	1.88	1.13

Note. — The blank spaces correspond to values of  $e_C$  and  $A_{\Delta t}$  for which the integrations were not continued beyond  $10^{10}$  seconds.



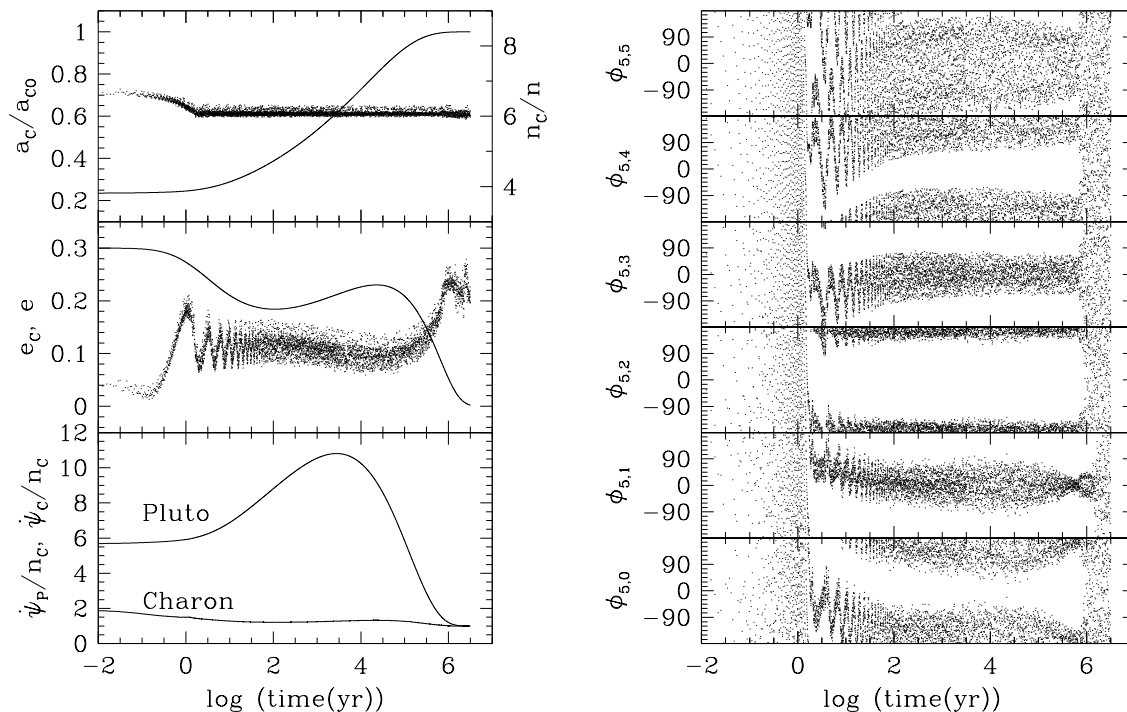


Fig. 3.— Example of a test particle that survives to the end of the tidal evolution of Pluto-Charon in the constant  $\Delta t$  model. The test particle is captured into simultaneous libration of all six resonance variables  $\phi_{5,l}$  at the 6:1 commensurability with Charon, with the orbits anti-aligned.  $e$  increases to above  $\approx 0.2$  with decreasing  $e_C$  as Pluto and Charon approach the dual synchronous state. Initial  $e_C = 0.3$  and  $A_{\Delta t} = 11$ .

remains significant. As  $a_C$  approaches  $17R_P$  and Charon and Pluto approach synchronous rotation, the test particle escapes from all six 6:1 resonances, but it stays near the 6:1 commensurability. However,  $e$  increases as  $e_C$  decreases on the approach of Pluto-Charon to the dual synchronous state. So even though the test particle is migrated successfully to the current semimajor axis of Hydra, it does not resemble the characteristics of Hydra’s orbit, because tides at its current semimajor axis are too weak to damp its eccentricity in the age of the Solar System (Stern et al. 2006).

The second tidal model we consider is the constant  $Q$  model. Details of this model are also given in paper I. The ratio of dissipation in Charon to that in Pluto for this model is given by

$$A_Q = \frac{k_{2C} Q_P}{k_{2P} Q_C} \left(\frac{M_P}{M_C}\right)^2 \left(\frac{R_C}{R_P}\right)^5 \approx \frac{\mu_P Q_P R_C}{\mu_C Q_C R_P}. \quad (5)$$

We use  $Q_P = 100$ , same as that in paper I. Again, a range of eccentricity evolution of Charon is explored with a combination of initial  $e_C$  and  $A_Q$ :  $A_Q = 0.55, 0.65,$  and  $0.75$  for initial  $e_C = 0.1$

Table 3. Fraction of captured test particles, in unit of permille (‰), after  $3 \times 10^{11}$  seconds in the constant  $Q$  model with  $C_{22i} = 0$ .

Initial $e_C$	$A_Q = 0.55$ or $1.13$			$A_Q = 0.65$ or $1.14$			$A_Q = 0.75$ or $1.15$		
	5:1	6:1	7:1	5:1	6:1	7:1	5:1	6:1	7:1
0.1	1.63	4.63	1.13	2.88	6.25	1.25	3.75	5.13	0.38
0.2	0.38	2.88	2.75	0.50	4.00	2.75	0.50	3.88	3.50
0.3	0.13	1.50	3.38	0.25	1.38	3.63	0	1.63	4.00

Note. — Larger  $A_Q$  for initial  $e_C = 0.3$  only.

Table 4. Fraction of survivors, in unit of permille (‰), to the end of the tidal evolution of Pluto-Charon in the constant  $Q$  model with  $C_{22i} = 0$ .

Initial $e_C$	$A_Q = 0.55$ or $1.13$			$A_Q = 0.65$ or $1.14$			$A_Q = 0.75$ or $1.15$		
	5:1	6:1	7:1	5:1	6:1	7:1	5:1	6:1	7:1
0.1	0	2.13	0.63	...	...	...	2.50	0.75	0
0.2	...	...	...	0.13	2.75	1.50	...	...	...
0.3	0	0	0.50	...	...	...	0	0.75	0.75

Note. — Larger  $A_Q$  for initial  $e_C = 0.3$  only. The blank spaces correspond to values of  $e_C$  and  $A_Q$  for which the integrations were not continued beyond  $3 \times 10^{11}$  seconds.

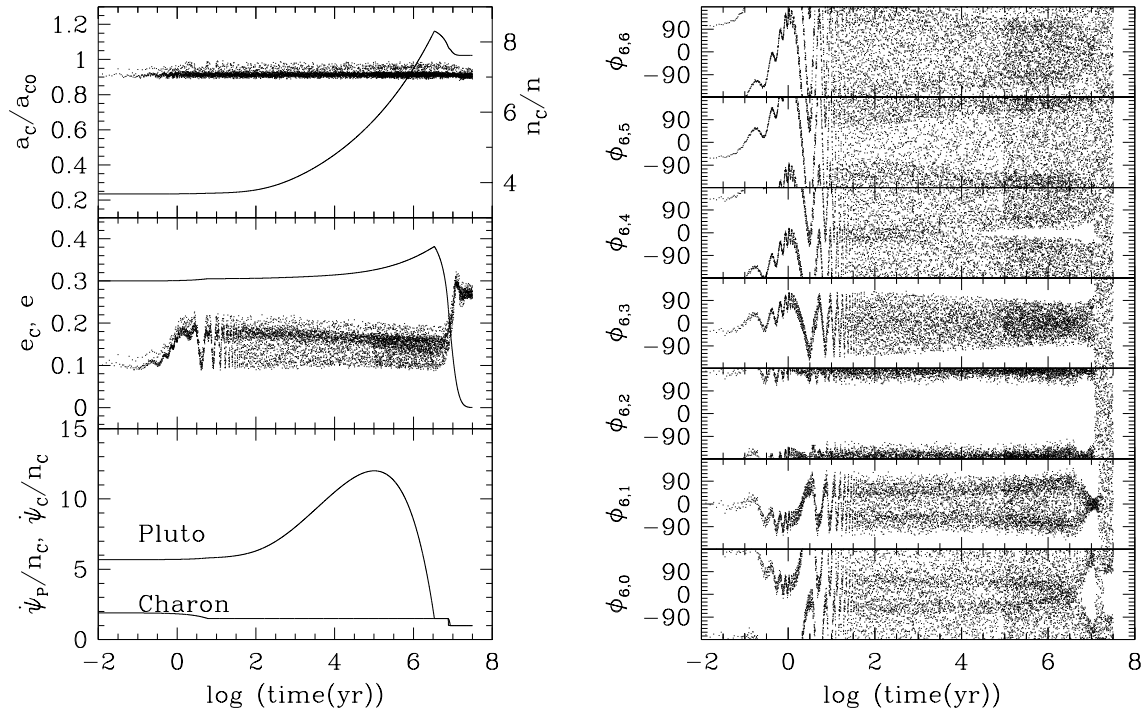


Fig. 4.— Example of a test particle that survives to the end of the tidal evolution of Pluto-Charon in the constant  $Q$  model. The test particle is captured and transported in multiple resonances at the 7:1 commensurability in an anti-aligned configuration with Charon.  $e$  increases as  $e_C$  decreases on the approach of Pluto-Charon to the dual synchronous state. Initial  $e_C = 0.3$  and  $A_Q = 1.13$ .

and 0.2, and  $A_Q = 1.13, 1.14,$  and  $1.15$  for initial  $e_C = 0.3$ . The resulting evolution of Charon’s orbit is displayed in paper I. The initial distribution of test particles is the same as the constant  $\Delta t$  model above. The first stage of integration ends after  $3 \times 10^{11}$  seconds ( $\approx 10^4$  years), when the orbit expansion (increase in  $a_c$ ) is comparable to that in the constant  $\Delta t$  model.

We consider first runs with  $C_{22i} = 0$ . Table 3 shows the statistics of test particles captured into multiple resonances with stable orbit expansion at the 5:1, 6:1, and 7:1 commensurabilities for the specified values of  $A_Q$  and initial  $e_C$  when the first stage of integration ends. Like the constant  $\Delta t$  model, there is a considerable number of captures and stable migration at the three commensurabilities, but none at the 3:1 or 4:1. Also like the constant  $\Delta t$  model, the fraction of captures into multiple 5:1 resonances decreases with increasing initial  $e_C$ , and the opposite happens for 7:1 resonances. The results of the continued integrations to the end of the tidal evolution of Pluto-Charon for the four corners and the middle point of the  $(e_C, A_Q)$  grid are presented in Table 4. More than one third of the survivors in the first stage remains. Despite the evolution timescale in the two tidal models differing by more than an order of magnitude, the capture statistics at the end of the first stage of our integration are within a factor of two, with the constant  $\Delta t$  model more

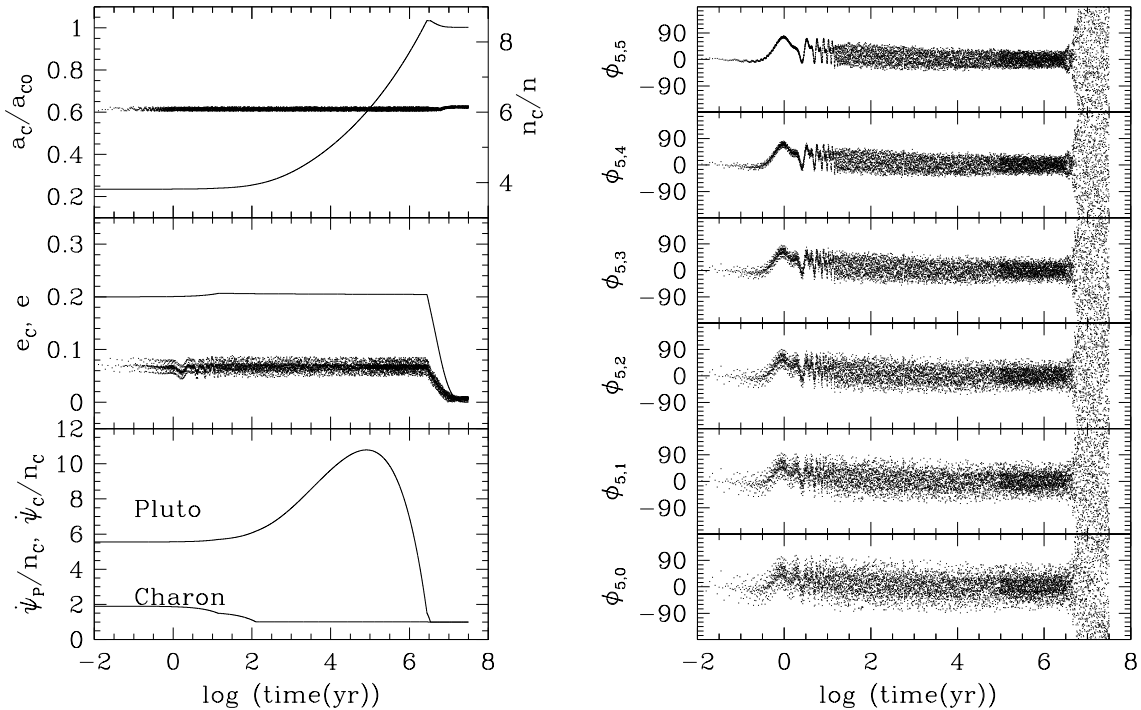


Fig. 5.— Only case where the test particle is captured and transported in an aligned configuration with Charon. The tidal model is constant  $Q$ , and all 6:1 resonance variables are librating about  $0^\circ$ . Note that in this case  $e$  damps to zero along with  $e_C$ . Initial  $e_C = 0.2$  and  $A_Q = 0.65$ .

effective for capture (compare Tables 1 and 3). On the other hand, the fraction of final survivors at the end of the tidal evolution in the constant  $Q$  model is more than that of constant  $\Delta t$  (compare Tables 2 and 4).

We have also repeated the runs with  $C_{22i} = 10^{-5}$  and the same values of  $A_Q$  as those with  $C_{22i} = 0$ . For initial  $e_C = 0.1$ , non-zero  $C_{22i}$  makes no difference in the tidal evolution of Pluto-Charon, and the test-particle statistics are comparable to those in Tables 3 and 4, but fluctuates due to stochastic capture. However, Charon is captured into 3:2 spin-orbit resonance for higher initial  $e_C$ . Charon’s eccentricity  $e_C$  quickly plummets for initial  $e_C = 0.2$ , and rises to  $e_C \gtrsim 0.36$ , where the evolution equations for constant  $Q$  are qualitatively inaccurate due to truncation of the expansion in orbital elements, for initial  $e_C = 0.3$  (see paper I). None of the test particles survives when  $e_C$  becomes too small for initial  $e_C = 0.2$  or too large for initial  $e_C = 0.3$ .

An example of a survivor in the constant  $Q$  model with  $C_{22i} = 0$  is shown in Fig. 4. The test particle is captured and transported in multiple resonances at the 7:1 commensurability in an anti-aligned configuration with Charon. This example is chosen to demonstrate the possibility of staying within the resonances when  $a_C$  is decreasing. If  $e_C$  is still large when  $a_C$  reaches the

current value, then by the conservation of angular momentum,  $a_C$  would overshoot before coming back to the current value when  $e_C$  decays. At the end of the integration, the test particle is in the  $l = 0$  resonance only, the coefficient of which does not involve  $e_C$ . We find that around half of the survivors in the two tidal models are in this situation, and the other half stay near the commensurabilities but no resonance variable is librating (e.g., Fig. 3). As in Fig. 3,  $e$  increases with decreasing  $e_C$  as Pluto and Charon approach the dual synchronous state.

Fig. 5 shows a case in the constant  $Q$  model with  $C_{22i} = 0$  where fortuitous initial conditions lead to all the resonance variables at the 6:1 commensurability librating about  $0^\circ$ , with the orbits being aligned ( $\varpi - \varpi_C = 0^\circ$ ). Unlike the evolution shown in Figs. 3 and 4, this example evolves with  $e$  decreasing to nearly zero with decreasing  $e_C$  as the dual synchronous rotation of Pluto-Charon is approached. This result might have been encouraging for the resonant transport of Pluto’s small satellites to their current positions. However, all of the 6:1 captures were for anti-aligned orbits except this one, which always lead to increase in  $e$  at the end of the tidal evolution of Pluto-Charon, and we could never capture a test particle into multiple resonances at the 3:1 and 4:1 commensurabilities. Finally, our assumption of  $J_{2P} = 0$  allowing similar rates of periaapse precession for Charon and the test particle cannot prevail. The effect of non-zero  $J_{2P}$  is explored in the next section.

### 3. EFFECT OF $J_{2P}$

After the impact that puts Charon in orbit around Pluto, Pluto would have absorbed a considerable fraction of the energy dissipated in the collision. The rapid rotation of a softened Pluto would lead to a nearly hydrostatic value of the zonal gravitational harmonic  $J_{2P}$ . For rotation about the axis of maximum moment of inertia, the changes in the principal components of Pluto’s moment of inertia tensor ( $\mathcal{A} \leq \mathcal{B} \leq \mathcal{C}$ ) from hydrostatic rotational distortion are (e.g., Peale 1973)

$$\begin{aligned} \Delta\mathcal{A} = \Delta\mathcal{B} &= -\frac{k_{fP}R_P^5\dot{\psi}_P^2}{9G}, \\ \Delta\mathcal{C} &= +\frac{2k_{fP}R_P^5\dot{\psi}_P^2}{9G}, \end{aligned} \tag{6}$$

where  $k_{fP}$  is the second degree fluid Love number. Then

$$J_{2P} = \frac{\Delta\mathcal{C} - (\Delta\mathcal{A} + \Delta\mathcal{B})/2}{M_P R_P^2} = \frac{k_{fP}R_P^3\dot{\psi}_P^2}{3GM_P}, \tag{7}$$

where we have neglected the tidal contribution to  $J_{2P}$  and any permanent deviation from axial symmetry. For  $a_C = 4R_P$ , the initial value of  $\dot{\psi}_P \approx 2\pi/(3.25 \text{ hours})$ , depending on the initial  $e_C$ , leading to  $J_{2P} \approx 0.17\text{--}0.26$  if  $k_{fP} \approx 1$  (by analogy with the Earth) to  $3/2$  (for homogeneous sphere). The neglected tidal contribution to  $J_{2P}$  is approximately 1% of this value. We also neglect the contributions of  $J_{4P}$  and  $J_{2P}^2$  to the evolution, since these contributions will only be significant when Charon is close to Pluto and they will only enhance the effect of  $J_{2P}$  on the orbital precessions.

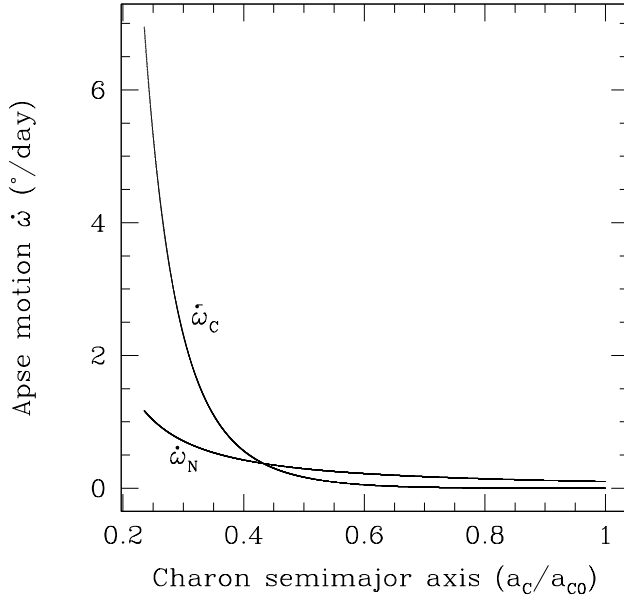


Fig. 6.— Periape precession rates of Charon and Nix for hydrostatic value of  $J_{2P}$  as a function of Charon’s semimajor axis. Nix is assumed to always be at the 4:1 mean-motion commensurability with Charon.

We have performed the non-zero  $J_{2P}$  counterparts of the test particle integrations presented in Section 2. An initial  $J_{2P} = 0.1$  is used, which decreases with  $\psi_P^2$  (see Eq. [7]), and the smaller effect of Charon’s  $J_2$  is ignored. The initial  $J_{2P}$  is smaller than the above estimate by a factor of  $\sim 2$  but large enough to demonstrate the effect of large  $J_{2P}$ . Only a few test particles survive the first stage out of all the integrations in the two tidal models and none of them can be migrated to the end of the tidal evolution of Pluto-Charon.

The periape precession rate (to the lowest order) of a satellite of Pluto is given by (Murray and Dermott 1999)

$$\dot{\omega} = \frac{3}{2}J_{2P}n \left(\frac{R_P}{a}\right)^2 + 2\alpha C_1(\alpha)n \frac{M_C}{M_P} \quad (8)$$

where the first term on the right hand side is the precession induced by Pluto’s  $J_2$  and the second term is the additional secular precession induced in the small satellite’s orbit due to Charon. In Eq. (8),  $n = [G(M_P + M_C)/a^3]^{1/2}$  is the orbital mean motion of the satellite whose precession is being determined,  $\alpha = a_c/a$ , and  $C_1(\alpha) = [2\alpha(d/d\alpha) + \alpha^2(d^2/d\alpha^2)]b_{1/2}^{(0)}/8$ , where  $b_{1/2}^{(0)}(\alpha)$  is the Laplace coefficient.

Fig. 6 illustrates the precession rates of Charon and Nix as a function of Charon’s semimajor axis, where Nix is assumed to always be at the 4:1 mean-motion commensurability with Charon. Only the  $J_{2P}$  term is applied to the precession of Charon. The nominal positions of the resonances

can be estimated by  $\dot{\phi}_{m,l} \approx 0$  or

$$n_{m,l} \approx \frac{n_C + l\dot{\omega}_C + (m-l)\dot{\omega}}{m+1}. \quad (9)$$

If  $J_{2P}$  (and hence  $\dot{\omega}_C$ ) are assumed to be zero, the resonances are close to each other, and the  $l = m$  corotation resonance is the first one being encountered when the orbit of Charon expands. With our estimated initial  $J_{2P} \approx 0.17$  (or larger),  $\dot{\omega}_C \gg \dot{\omega}$  at the 4:1 commensurability and the resonances are far apart, which means that it is much more difficult to librate simultaneously in multiple resonances. Also, the order of the resonances is reversed and the corotation resonance is the last one to be encountered. The resonances exchange their positions when  $J_{2P}$  decreases with  $\dot{\psi}_P^2$  as Charon moves outward, and any particles that were captured into multiple resonances become unstable. Secular precession due to Charon around the 5:1 and 6:1 commensurabilities should be smaller and the above arguments are applicable. It is now clear why the condition of similar precession rates for the simultaneous capture into and migration within multiple MMR at the 4:1 to 6:1 commensurabilities cannot be satisfied. This failure is compounded by the requirement that the synchronous precession rates must apply simultaneously to all of the small satellites if they are to be transported within multiple resonances.

#### 4. INTEGRATIONS WITH MASSIVE NIX AND HYDRA

Nix and Hydra could be affected by their proximity to the 3:2 mean-motion commensurability if they have non-zero masses. To see if we overlooked any possible capture into some resonance configuration that allows Nix and Hydra to be pushed to their current distances as Charon’s orbit tidally expands, we explore the effects of non-zero masses for Nix and Hydra. We ignore Kerberos and Styx in these simulations, as they are likely much smaller than Nix and Hydra (see footnote 1).

Here we use the Bulirsch-Stoer integrator with the constant  $\Delta t$  tidal model described in paper I. For the constant  $\Delta t$  model, the equations of motion in Cartesian coordinates with the instantaneous tidal forces and torques and the effects of  $J_{2P}$  and  $C_{22i}$  can be integrated directly (see paper I for details). As in the previous sections,  $k_{2P} = 0.058$ ,  $\Delta t_P = 600$  s, and the initial semimajor axis for Charon’s orbit is assumed to be  $a_C = 4R_P$  for all of the trials. We adopt  $A_{\Delta t} = 9$ . The initial spin angular velocity of Pluto is determined by the initial eccentricity of Charon’s orbit, consistent with the current total angular momentum of the Pluto-Charon system. Charon’s spin contributes relatively little to the total angular momentum, so we arbitrarily choose Charon’s initial spin angular velocity to be half that of Pluto. The initial angular momenta of Nix and Hydra are neglected in determining the initial conditions of Pluto and Charon.

Tholen et al. (2008) assign albedos of 0.08 and 0.18 to Nix and Hydra using their best fit masses ( $5.8 \pm 5.1 \times 10^{17}$  kg and  $3.2 \pm 6.3 \times 10^{17}$  kg, respectively) and assuming Charon’s density ( $1.63 \text{ g cm}^{-3}$ ) for both satellites. The uncertainties in the masses of Nix and Hydra exceed or are

comparable to their best fit values, so we choose to minimize the masses by assuming that Nix and Hydra have the same albedo as Charon of 0.34. With albedos of 0.34, the radii are reduced by factors of  $\sqrt{0.34/0.08} \approx 2$  and  $\sqrt{0.34/0.18} \approx 1.4$ , respectively, thereby reducing the masses by factors of  $\sim 8$  and  $\sim 3$ . These reductions in the masses from the Tholen et al. (2008) best fit values lead to  $M_N = 7.25 \times 10^{16}$  kg and  $M_H = 1.1 \times 10^{17}$  kg. These masses are between the high-albedo masses adopted by Lee and Peale (2006) and the upper limits derived by Youdin et al. (2012) from the orbital stability of Kerberos. By using minimum masses for Nix and Hydra, we maximize the chances for a stable configuration.

Initial semimajor axes of Nix and Hydra place them outside the 4:1 and 6:1 mean-motion commensurabilities with Charon, and Hydra outside the 3:2 commensurability with Nix ( $a_N > 2.52a_C$ ,  $a_H > 1.31a_N$ ). Eight initial values of  $e_C$  are chosen (0.02 to 0.30 at intervals of 0.04), six values of  $a_N/a_{C0}$  (0.60 to 0.70 at intervals of 0.02, where  $a_{C0} = 19573$  km is the current semimajor axis of Charon), six values of  $a_H/a_N$  (1.40, 1.42, 1.44, 1.45, 1.46, and 1.48), and 36 values of the initial true anomalies for both Nix and Hydra at intervals of  $10^\circ$ . Initial values of  $e_N = e_H = 0.01$ . The initially small values of  $e_N$  and  $e_H$  mean the periape positions of both Nix and Hydra will be rapidly scrambled by the perturbations, so initial values are arbitrary set at  $\varpi_N = 180^\circ$ , and  $\varpi_H = 0^\circ$ , for all the runs. Also, the initial value of  $\varpi_C = 0^\circ$  for all the runs, where this longitude will initially precess rapidly ( $\sim 5^\circ/\text{day}$ ) for hydrostatic value of  $J_{2P}$ . The choices of the parameter values lead to  $8 \times 6 \times 6 \times 36 \times 36 = 373,248$  trials for  $J_{2P} = 0$  and an equal number of trials for hydrostatic value of  $J_{2P}$  ( $= 0.17$  initially and decreasing with  $\dot{\psi}_P^2$ ; see Eq. [7]). A run is terminated if any eccentricity exceeds 0.7 or any semimajor axis exceeds  $5a_{C0}$ .

There are no survivors for either value of  $J_{2P}$ . The longest time to instability is a little over  $10^5$  days, where longer times to instability corresponded to smaller values of the initial  $e_C$ . With  $J_{2P} = 0$  one could hope that there might be capture of Nix into multiple resonances with subsequent stable expansion — at least until the 6:1 commensurability with Hydra is encountered. But recall that we get no such captures when Nix is a test particle (Section 2), and that result seems to apply with finite masses. Apparently Nix only gets caught into a single MMR, never the corotation resonance, with subsequent increase in the eccentricity to the point of instability, as for the case where  $J_{2P}$  is the hydrostatic value.

Fig. 7 shows the evolution to instability for a typical integration with hydrostatic value of  $J_{2P}$ . Panel A shows the evolution of the semimajor axes of Charon, Nix and Hydra, and Panel B shows Charon’s and Pluto’s spin histories. Charon’s orbit expands as both Pluto’s and Charon’s spins decrease. Charon’s spin decreases rapidly toward the asymptotic spin state, which is a little faster than the synchronous spin. Continued evolution would trap Charon into synchronous rotation relatively early unless the eccentricity increases. Nix’s semimajor axis is unaffected at first except for short period fluctuations, but it starts to rise near 1400 days as a result of being trapped into a 4:1 MMR, where the resonance variable  $\phi_{3,1} = 4\lambda_N - \lambda_C - \varpi_C - 2\varpi_N$  is librating. The semimajor axis of Nix’s orbit must increase while the resonance variable is librating in order to preserve the 4:1 commensurability as Charon’s orbit continues to expand. The value of the ratio  $n_C/n_N$  stops



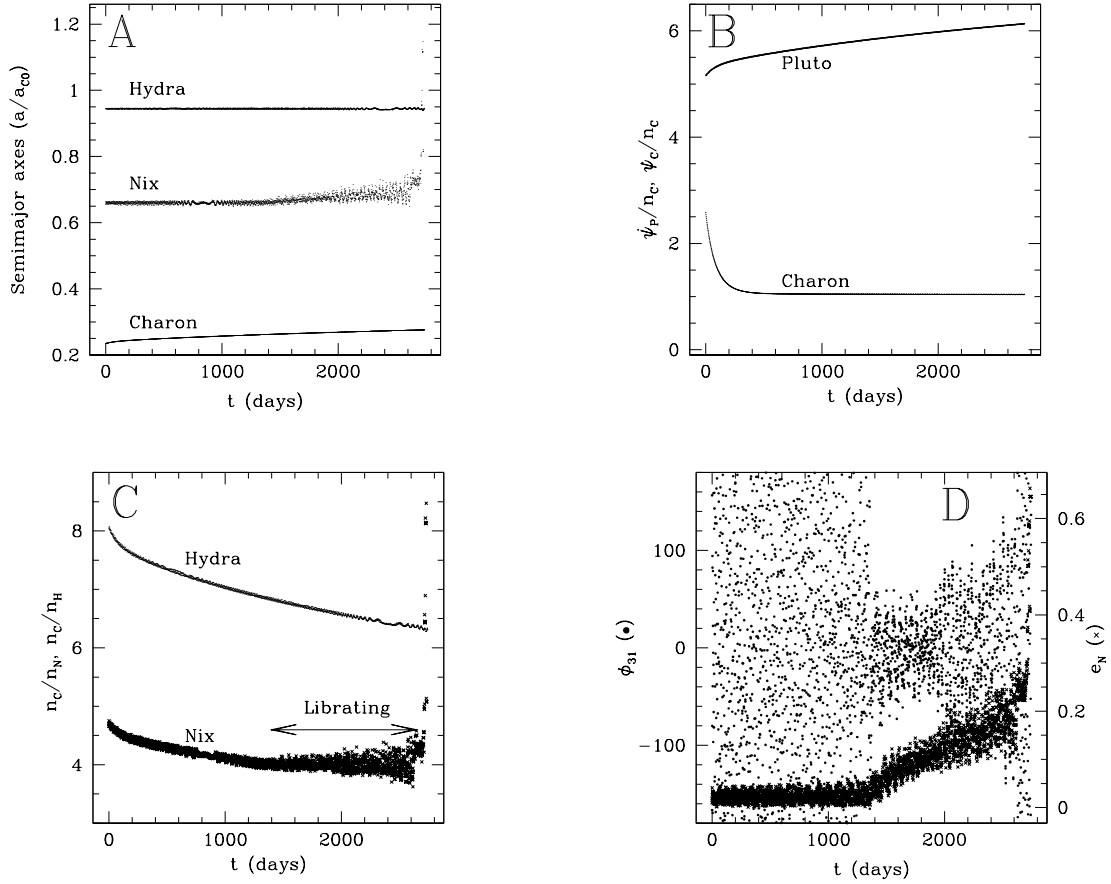


Fig. 7.— Typical evolution to instability during expansion of Charon’s orbit for simulations with massive Nix and Hydra. The tidal model is constant  $\Delta t$ , and  $J_{2P}$  has hydrostatic value. Initial conditions:  $e_C = 0.06$ ,  $a_N = 0.66a_{C0}$ ,  $a_H = 1.43a_N$ ,  $f_N = 230^\circ$ ,  $f_H = 330^\circ$ .

decreasing at 4:1 near 1400 days as shown in Panel C. Panel D shows the libration of the resonance variable  $\phi_{3,1}$  starting near 1400 days, which libration persists until about 2600 days. Also shown in Panel D is the rapid increase in Nix’s eccentricity as Nix’s orbit is pushed outward by the resonant interaction with Charon. This increase in  $e_N$  is as expected for evolution within any single Lindblad resonance (see Section 1). Simultaneous with the increase in  $e_N$ , we see in Panel D that the amplitude of libration increases to the point where the resonance variable begins circulating, and instability ensues shortly thereafter with the sudden growth of both  $e_N$  and  $a_N$ .

During all of this activity with Nix, Hydra’s semimajor axis is almost undisturbed until oscillations are induced because of the closer encounters with Nix as the latter’s eccentricity grows. This relatively mild disturbance is shown in both Panels A and C near the right extremes of the Hydra curves. As the 4:1 mean-motion commensurability between Charon and Nix is always encountered before the 6:1 commensurability of Charon and Hydra, it is always Nix that destroys the stability of the system as Charon’s orbit expands.

Since Hydra’s orbit is almost undisturbed in the above example, we repeat the calculation with the same set of parameters but with Hydra’s semimajor axis starting out closer to the 3:2 MMR with Nix to see if the proximity of this resonance could influence the outcome of the multi-parameter trial with otherwise the same parameters. With hydrostatic value of  $J_{2P}$ , there again are no survivors for two runs with the closest initial values of semimajor axes of  $a_H = 1.34a_N$  and  $1.31a_N$ , respectively, where the latter value is just outside the 3:2 MMR.

We are also able to start a calculation with Hydra and Nix in a single MMR at the 3:2 mean-motion commensurability with  $3\lambda_H - 2\lambda_N - \varpi_H$  librating about  $180^\circ$  with amplitude  $\sim 20^\circ$ . The latter is established by applying an artificial drag opposing the velocity of Hydra to ease it into the 3:2 MMR with Nix, with the tidal expansion of Charon’s orbit turned off. We could only get capture into this particular resonance at the 3:2 commensurability. The purpose of this exercise is to see if the pre-existence of a Nix-Hydra 3:2 MMR could lead to a stable expansion of the orbits after all. With initial conditions in the above 3:2 resonance, the tidal expansion of Charon’s orbit leads to instability rather quickly, but not by Hydra’s eccentricity increasing because it is in the single 3:2 MMR, but by Charon’s perturbations of Nix as before — almost as if Hydra were not there. Nix gets briefly into a single 4:1 Lindblad resonance with Charon, with rapidly increasing eccentricity and ultimate instability. So whether or not Hydra is in a 3:2 resonance with Nix, it is Charon’s perturbations of Nix that lead to the instability.

Finally, although  $\Delta t_P = 600$  s is similar to that for the Earth (see paper I), there is some risk that artifacts can be introduced if  $\Delta t_P$  is too large and the rate of evolution is too fast. Interestingly, calculations with the same initial conditions as those for Fig. 7 above, but with  $\Delta t_P$  decreased by one, two and three orders of magnitude, produce the same overall evolution with capture of Nix into the 4:1 MMR described above at about the same value of Charon’s semimajor axis  $a_C$ . However, instability ensues at progressively smaller values of  $a_C$  as  $\Delta t_P$  is decreased, with instability occurring just as Charon reached the 4:1 commensurability with Nix when  $\Delta t_P = 0.6$  s.

The perturbations by the massive Charon accumulate as Charon spends longer times near a given semimajor axis, leading to the “earlier” instability.

## 5. CONCLUSIONS AND DISCUSSION

We have found what we think is the first demonstration of the stable expansion of a test particle’s orbit captured into multiple resonances at the same mean-motion commensurability with an inner satellite (i.e., Charon), whose orbit is expanding. The test particle’s orbital eccentricity  $e$  does not grow excessively, as occurs when captured only into a single Lindblad resonance containing  $e$  in the coefficient of the restoring torque. The hope that such captures would allow the resonant transport of the small satellites of Pluto and thereby avoid the problem of unlikely capture into the corotation resonances only (where  $e$  would not grow with continued evolution) was shattered by several observations: (1) While we could stably migrate a test particle at the 5:1, 6:1 and 7:1 commensurabilities in multiple resonances, we could never stably migrate a test particle at the 3:1 and 4:1 commensurabilities. (2) For the test particles stably captured into an orbital configuration anti-aligned with Charon, final  $e$  is too large as  $e$  increases with decreasing  $e_C$  on the approach of Pluto-Charon to the dual synchronous state. (3) There is only one fortuitous selection of initial conditions for the constant  $Q$  model that leads to the test particle’s eccentricity damping to zero with  $e_C$ . This test particle is captured into an aligned configuration at the 6:1 commensurability. Our results suggest that the eccentricity evolution in multiple resonances is related to the geometry of the resonances, with the evolution following that of Charon in the aligned configuration and opposite evolution for the anti-aligned configuration, but a better theoretical understanding of the evolution of test particles in multiple resonances is needed. (4) The requirement that Pluto’s  $J_{2P} = 0$  for  $\dot{\varpi}_C \approx \dot{\varpi}$ , for either anti-aligned or aligned orbits, does not prevail. The differential precession of the longitude of periapse of a test particle and that of Charon for a hydrostatic value of  $J_{2P}$  precludes capture into multiple resonances at the same commensurability.

To check the parameter space for possible oversight of a stable, migrating configuration, we integrated the Pluto-Charon system with finite but minimal masses of Nix and Hydra for a wide range of plausible initial parameter values that would allow encounter of the 4:1 and 6:1 mean-motion commensurabilities between Charon and Nix and Charon and Hydra, respectively. Out of more than  $3.7 \times 10^5$  trials for  $J_{2P} = 0$  and an equal number of trials for hydrostatic value of  $J_{2P}$ , none of the systems survives. Placing Hydra closer to or even in the 3:2 resonance with Nix, or increasing the timescale for the expansion of Charon’s orbit, did not help. So we conclude that the transport of the small satellites in MMR to their current distances from Pluto as Charon’s orbit tidally expanded is not possible.

Is there an alternative origin? Lithwick and Wu (2008) have proposed the creation of a debris disk close to the current locations of the small satellites after the tidal evolution of Pluto-Charon was complete. Such a debris disk, if sufficiently collisional, would settle down into the plane of the orbit of Charon, where it could accrete into larger bodies and/or sort the existing debris

into long-term stable orbits. Pires dos Santos et al. (2012) have shown that some planetesimals could be temporarily captured from heliocentric orbits into orbits around Pluto-Charon due to the binary nature of Pluto-Charon, with the capture lifetime  $\sim 100$  years. A debris disk could be formed if the temporarily captured planetesimals collided with other planetesimals on heliocentric orbits. However, for planetesimals large enough to have sufficient mass to form the small satellites, Pires dos Santos et al. (2012) estimated that a collision during temporary capture is extremely unlikely, because the timescale for collision is many orders of magnitudes longer than the capture lifetime.

Alternatively, Kenyon and Bromley (2014) have suggested that the small satellites grew close to their current locations from debris ejected by the Charon-forming impact *before* any significant tidal expansion of Charon’s orbit. The debris from the impact was initially located at distances less than  $\sim 30R_P$  (Canup 2011), but Kenyon and Bromley (2014) argued that the debris would first evolve into a ring at  $\sim 20R_P$  and then spread out into a disk out to  $\sim 60R_P$ . However, if the small satellites formed this way, they would likely suffer the same problem seen in Section 2 with the subsequent tidal expansion of Charon’s orbit. For example, if a small satellite formed near the current location of Nix at  $\approx 43R_P$ , it would encounter the 7:1 to 5:1 mean-motion commensurabilities with Charon when  $a_C \approx 11.8\text{--}14.7R_C$  or  $a_C/a_{C0} \approx 0.69\text{--}0.86$ . For Charon at these distances, the effect of  $J_{2P}$  on its precession rate is likely small (see Fig. 6). Therefore, when the small satellite encountered one of these commensurabilities, its orbit would evolve as shown in Section 2 and would become either unstable or too eccentric after stable multi-resonance capture and transport. It is unclear whether these problems could be overcome if the ratio of tidal dissipation ( $A_{\Delta t}$  or  $A_Q$ ) was much larger than what we have assumed and Charon’s orbit circularized rapidly or if the orbits of the small satellites could be circularized by interactions with any remaining debris.

Since none of the proposed scenarios appears viable yet, the origin of the small satellites of Pluto remains a mystery and further investigations are needed. The upcoming *New Horizons* flyby may reveal new clues and constraints.

The authors are grateful for the support of a Postgraduate Studentship at the University of Hong Kong (WHC), Hong Kong RGC Grant HKU 7024/08P (WHC and MHL), and the NASA Planetary Geology and Geophysics Program under Grant NNX08AL76G (SJP). They appreciated useful discussions with Robin Canup, Yoram Lithwick, and Yanqin Wu.

## REFERENCES

- Beust, H., 2003. Symplectic integration of hierarchical stellar systems. *Astron. Astrophys.* 400, 1129–1144.
- Buie, M.W., Grundy, W.M., Tholen, D.J., 2013. Astrometry and Orbits of Nix, Kerberos, and Hydra. *Astron. J.* 146, 152.
- Canup, R.M., 2005. A giant impact origin of Pluto-Charon. *Science* 307, 546–550.
- Canup, R.M., 2011. On a Giant Impact Origin of Charon, Nix, and Hydra. *Astron. J.* 141, 35.
- Cheng, W.H., Lee, M.H., Peale, S.J., 2014. Complete tidal evolution of Pluto-Charon. *Icarus* 233, 242–258.
- Christy, J.W., Harrington, R.S., 1978. The satellite of Pluto. *Astron. J.* 83, 1005–1008.
- Kenyon, S.J., Bromley, B.C., 2014. The Formation of Pluto’s Low-mass Satellites. *Astron. J.* 147, 8.
- Lee, M.H., Peale, S.J., 2003. Secular Evolution of Hierarchical Planetary Systems. *Astrophys. J.* 592, 1201–1216.
- Lee, M.H., Peale, S.J., 2006. On the orbits and masses of the satellites of the Pluto Charon system. *Icarus* 184, 573–583.
- Leung, G.C.K., Lee, M.H., 2013. An Analytic Theory for the Orbits of Circumbinary Planets. *Astrophys. J.* 763, 107.
- Levison, H.F., Duncan, M.J., 1994. The long-term dynamical behavior of short-period comets. *Icarus* 108, 18–36.
- Lithwick, Y., Wu, Y., 2008. On the Origin of Pluto’s Minor Moons, Nix and Hydra. preprint (arXiv:0802.2951) .
- Murray, C.D., Dermott, S.F., 1999. *Solar System Dynamics*. Cambridge Univ. Press, Cambridge.
- Nagy, I., Süli, Á., Érdi, B., 2006. A stability study of Pluto’s moon system. *Mon. Not. R. Astron. Soc.* 370, L19–L23.
- Peale, S.J., 1973. Rotation of solid bodies in the solar system. *Rev. Geophys. Space Phys.* 11, 767–793.
- Peale, S.J., Cheng, W.H., Lee, M.H., 2011. The Evolution of the Pluto System. EPSC-DPS Joint Meeting 2011 , 665.

- Pires Dos Santos, P.M., Giuliatti Winter, S.M., Sfair, R., 2011. Gravitational effects of Nix and Hydra in the external region of the Pluto-Charon system. *Mon. Not. R. Astron. Soc.* 410, 273–279.
- Pires dos Santos, P.M., Morbidelli, A., Nesvorný, D., 2012. Dynamical Capture in the Pluto-Charon System. *Celest. Mech. Dyn. Astron.* 114, 341–352.
- Showalter, M.R., Hamilton, D.P., Stern, S.A., Weaver, H.A., Steffl, A.J., Young, L.A., 2011. New Satellite of (134340) Pluto: S/2011 (134340) 1. *IAU Circ.* 9221.
- Showalter, M.R., Weaver, H.A., Stern, S.A., Steffl, A.J., Buie, M.W., Merline, W.J., Mutchler, M.J., Soummer, R., Throop, H.B., 2012. New Satellite of (134340) Pluto: S/2012 (134340) 1. *IAU Circ.* 9253.
- Stern, S.A., Parker, J.W., Duncan, M.J., Snowdall, Jr., J.C., Levison, H.F., 1994. Dynamical and observational constraints on satellites in the inner Pluto-Charon system. *Icarus* 108, 234–242.
- Stern, S.A., Weaver, H.A., Steffl, A.J., Mutchler, M.J., Merline, W.J., Buie, M.W., Young, E.F., Young, L.A., Spencer, J.R., 2006. A giant impact origin for Pluto’s small moons and satellite multiplicity in the Kuiper belt. *Nature* 439, 946–948.
- Tholen, D.J., Buie, M.W., Grundy, W.M., Elliott, G.T., 2008. Masses of Nix and Hydra. *Astron. J.* 135, 777–784.
- Ward, W.R., Canup, R.M., 2006. Forced resonant migration of Pluto’s outer satellites by Charon. *Science* 313, 1107–1109.
- Weaver, H.A., Stern, S.A., Mutchler, M.J., Steffl, A.J., Buie, M.W., Merline, W.J., Spencer, J.R., Young, E.F., Young, L.A., 2006. Discovery of two new satellites of Pluto. *Nature* 439, 943–945.
- Wisdom, J., Holman, M., 1991. Symplectic maps for the n-body problem. *Astron. J.* 102, 1528–1538.
- Youdin, A.N., Kratter, K.M., Kenyon, S.J., 2012. Circumbinary Chaos: Using Pluto’s Newest Moon to Constrain the Masses of Nix and Hydra. *Astrophys. J.* 755, 17.